DEVELOPMENT OF A NEW APPROACH FOR THE PREDICTION OF PATTERN TRANSITION OF TWO-PHASE STRATIFIED FLOW IN DUCTS AND PIPES

Daniel Rodríguez, dani@mec.uff.br, danielrodalv84@gmail.com[1,2]
Elmer Mateus Gennaro, elmer.gennaro@sjbv.unesp.br[3]

[1]Laboratory of Theoretical and Applied Mechanics (LMTA), Graduate program in Mechanical Engineering (PGMEC), Department of Mechanical Engineering, Universidade Federal Fluminense, Niterói, RJ 24210-240 Brazil
[2]Pontifical Catholic University of Rio de Janeiro (PUC-RJ), R. Marques de São Vicente 225-Gávea, Rio de Janeiro, 22451-900, Brazil
[3]São Paulo State University UNESP, Campus São João da Boa Vista, SP 13874-149, Brazil

Abstract: *This contribution presents the most recent steps in the development of a new approach for the prediction of flow pattern transitions from steady, smooth stratified flow to wavy stratified, and towards the emergence of slugs or pistons. The true three-dimensional description of the flow field is considered into a multidimensional, linear instability eigenproblem, that eliminates the constrains associated with both the one-dimensional two-fluids model and the Orr-Sommerfeld equation, by introducing the real two-dimensional cross-section geometry. Use of modern computational and algorithmic techniques are instrumental in the successful implementation of the proposed approach. Optimized sparse linear algebra for high-order spatial discretizations and shared-memory parallelization enable us to compute the three-dimensional, unsteady velocity fields in a laptop computer.*
Keywords: *Multiphase flows, Hydrodynamic Stability, Numerical Methods*

1. INTRODUCTION

Technological problems in which two or more fluids flow concurrently along channels, pipes or ducts with different cross-sections are present in many fields of engineering, like chemical process or oil extraction. The ability of predicting the flow pattern for given configuration and operation conditions is of the utmost importance, due to their significant effect on the global magnitudes of interest for the designer, e.g. pressure losses along duct, drag forces, duct-walls heating, etc. One of such pattern transitions occurs in horizontal or inclined ducts as the flow rate of one or the two phases is gradually increased from relatively low values; the flow then evolves from a steady stratified regime, with smooth interface, towards a wavy stratified regime, in which the interface presents short-wavelength roughness, long waves comparable to the duct cross-section, or a combination of both. If long waves grow enough in amplitude, eventually the cross-section will be bridged by one of the two fluids, and transition may occur to a new pattern, dominated by slugs. Consensus exists in the literature on pointing out interfacial instability as responsible for this transition.

The most generally accepted methods used in the prediction of interfacial instabilities in confined two-phase flows evolved from the one-dimensional two-fluids model (Taitel and Dukler (1976); Lin and Hanratty (1986); Barnea and Taitel (1993)), which assumes a simplified form of the velocity profiles and derives a momentum conservation equation based on averaging the flow properties over cross-sections. The reason of the success of this method relies on the necessity of introducing heuristic correlations for the wall and interfacial friction factors which, once calibrated with experiments, can deliver reasonable predictions in a great variety of flows. On the other hand, methods derived from first-principles for understanding the physical processes associated with interfacial instabilities, like those presented by Renardy (1987) or Boomkamp and Miesen (1997), have not been applied in the same degree as the one-dimensional two-fluids model, due to their higher computational expenditure. These methods consider the discretized momentum equations for each phase separately, coupled through interfacial conditions, to produce an eigenvalue problem for one-dimensional disturbances. Consequently, this methodology is limited to simple flows like plane channels our concentric annular flows.

This contribution presents recent achievements in the development of a methodology that enables the stability analysis of separated-phases flow along ducts and pipes of arbitrary cross section, without resorting to the simplifications of the existing approaches. The real duct section geometry and three-dimensional nature of the flow field is taken into account, and the three-dimensional momentum equations are discretized in a couple manner to yield an eigenvalue problem for the streamwise growth or decay of instability waves. The spatial structure of their velocity field is fully determined by eigenfunctions which depend in an inhomogeneous manner on the two cross-plane directions, and have a wave-like behavior in the streamwise direction and time. This approach enables the introduction from first principles, for the first time, of the following aspects: (i) cross-sectional duct geometries and base velocity fields with dependence on two spatial directions, (ii) arbitrary interface topology, and (iii) three-dimensional secondary flows induced by instabilities.

2. MATHEMATICAL MODELING

The mathematical model for the confined two-phase flow within pipes is based on the complete Navier-Stokes equations in differential form. A single-fluid method along with an interface-capturing level-set approach is used here to

describe the fluid motion, as described next.

Equations are non-dimensionalized using the following magnitudes: a length characteristic of the duct cross section, e.g. the channel width or pipe diameter D^*; a characteristic velocity in one of the phases U_1^*, typically the less dense one; the corresponding density and molecular viscosity in the same phase, ρ_1^* and μ_1^*; a characteristic convection time D^*/U_1^*; and the dynamic pressure on phase 1, $\rho_1^* U_1^{*2}$. Denoting the gravity acceleration by g^* and the surface tension coefficient between the two phases by σ^*, the following dimensionless quantities are formed:

$$\chi = \frac{\rho_2^*}{\rho_1^*}, \quad \eta = \frac{\mu_2^*}{\mu_1^*}, \quad Re = \frac{\rho_1^* U_1^* D^*}{\mu_1^*}, \quad We = \frac{\rho_1^* U_1^{*2} D^*}{\sigma^*} \quad \text{and} \quad Fr = \frac{U_1^*}{\sqrt{g^* D^*}}. \tag{1}$$

In this dimensionless form, the momentum and mass conservation equations can be written as

$$\rho \frac{\partial \mathbf{v}}{\partial t} + \rho \mathbf{v} \cdot \nabla \mathbf{v} = -\nabla p + \frac{1}{Re} \nabla \cdot (2\mu \mathbf{D}) + \frac{1}{We} \mathbf{T} + \frac{1}{Fr^2} \mathbf{g}, \quad \text{and} \quad \nabla \cdot \mathbf{v} = 0, \tag{2}$$

where $\mathbf{D} = (\partial u_i/\partial x_j + \partial u_j/\partial x_i)/2$ is the velocity gradient tensor, $\mathbf{T}$ is a volume force modeling the surface tension and $\mathbf{g}$ is the unitary vector pointing in the direction of gravity.

A level set method (Sussman *et al.* (1994)) is employed here in order to capture the fluid interface and track its deformation without incurring in heavy computational costs. A scalar function ϕ is defined such that $\phi = 0$ at the interface, $\phi > 0$ at phase 1 and $\phi < 0$ at phase 2. The evolution of the scalar level-set function is governed by

$$\frac{\partial \phi}{\partial t} + \mathbf{v} \cdot \nabla \phi = 0. \tag{3}$$

After introduction of ϕ, the density and viscosity spatial distributions are expressed as

$$\rho = H(\phi) + \chi(1 - H(\phi)), \quad \text{and} \quad \mu = H(\phi) + \eta(1 - H(\chi)), \tag{4}$$

where H is the Heaviside function.

Provided that $\phi = 0$ defines the interface location, the interface local normal vector, curvature and surface tension are defined as

$$\mathbf{n} = -\frac{\nabla \phi}{|\nabla \phi|}, \qquad \kappa(\phi) = \nabla \cdot \left(\frac{\nabla \phi}{|\nabla \phi|} \right), \quad \text{and} \quad \mathbf{T} = \kappa(\phi)\delta(\phi)\mathbf{n} = -\delta(\phi) \nabla \cdot \left(\frac{\nabla \phi}{|\nabla \phi|} \right) \frac{\nabla \phi}{|\nabla \phi|}, \tag{5}$$

where the Dirac delta function δ has been used. The fluid flow described by equations (2), and (3) is represented in vector form as $\mathbf{q} = [\mathbf{v}\ p\ \phi]^T$, and is a function of the three spatial directions (x denoting the axial direction and y and z denoting the cross-sectional ones) and time t. Following Reynolds decomposition, the flow is divided into a time-independent *mean* flow $\bar{\mathbf{q}}$ and a fluctuation component $\mathbf{q}'$:

$$\mathbf{q} = \bar{\mathbf{q}}(\mathbf{x}) + \mathbf{q}'(\mathbf{x}, t). \tag{6}$$

The mean flow $\bar{\mathbf{q}}$ can represent a steady solution of the governing equations or a time-averaged flow obtained from time-accurate numerical simulations, Reynolds-averaged Navier-Stokes (RANS) simulations or experimental measurements. Upon substitution of equation (6) on the governing equations (2), and (3), two systems of equations are obtained respectively for the mean flow and fluctuations. These two systems are coupled by both linear and nonlinear interactions, and its accurate solution would require of large numerical computations (e.g. Gada and Sharma (2012)). The characteristics of the flow under consideration can be exploited in order to introduce simplifications in the governing equations, that allow us to obtain solutions in a very efficient manner. These simplifications are discussed next.

2.1 Fully-developed flow along three-dimensional ducts and pipes

A necessary step in the stability analysis is the determination of an adequate base flow, i.e., a time-independent flow field representative of the undisturbed flow conditions. For analyses based on one-dimensional velocity profiles (Renardy, 1987; Boomkamp and Miesen, 1997), such a base flow is obtained analytically. For general two-dimensional cross-sections a numerical procedure needs to be developed.

Let y and z be the cross-plane and x the streamwise directions. Gravity acts on the negative y direction, so that the heavier fluid occupies the region with lower y coordinates. Capillarity effects are neglected in the base flow, so that the interface is localized at a constant $y = h_{in}$ location. Assuming fully-developed flow, $\bar{v} = \bar{w} = 0$ and $\partial \bar{\mathbf{q}}/\partial x = 0$. The only non-trivial governing equation is then the streamwise momentum one, which reads:

$$Re \frac{\partial \bar{p}}{\partial x} = \frac{\partial}{\partial y} \left(\bar{\mu} \frac{\partial \bar{u}}{\partial y} \right) + \frac{\partial}{\partial z} \left(\bar{\mu} \frac{\partial \bar{u}}{\partial z} \right), \tag{7}$$

which is complemented with no-slip conditions at the solid walls.

In experiments, the easily controllable variables are not the pressure gradient or the interface height, but the mass flux rates of each phase. Taking advantage of the Heaviside functions, these flux rates are written as

$$G_1 = \int \int \bar{\rho} \bar{u} H \mathrm{d}y \mathrm{d}z, \quad G_2 = \int \int \bar{\rho} \bar{u} (1 - H) \mathrm{d}y \mathrm{d}z. \tag{8}$$

Table 1: Axial pressure gradient $S = \partial\bar{p}/\partial x$, interface height h_{in} and peak streamwise velocity U_{max} for different aspect ratios.

	-$S \times 10^2$	h_{in}	W_{max}
Channel (analytic)	-2.2915	0.5581423283	1.7438687976
Channel (Numeric)	-2.3430	0.5571131872	1.7502851147
Duct $L_x = 200$	-2.3489	0.5570754489	1.7550364001
Duct $L_x = 100$	-2.3543	0.5570374683	1.7594621524
Duct $L_x = 50$	-2.3654	0.5569565480	1.7684297006
Duct $L_x = 20$	-2.4003	0.5566724882	1.7961604078
Duct $L_x = 10$	-2.5245	0.5536195037	1.8542023566
Duct $L_x = 5$	-2.6536	0.5526641926	1.9584841230
Duct $L_x = 2$	-3.2980	0.5435924303	2.2768876665
Duct $L_x = 1$	-5.0368	0.5226276737	2.5926535642
Duct $L_x = 0.5$	-11.9384	0.4714249674	2.9906203244

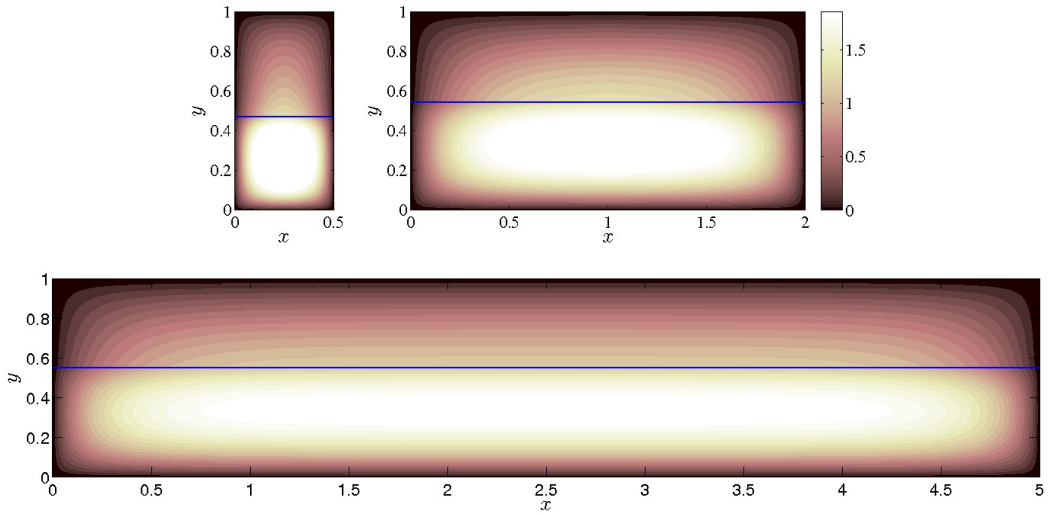

Figure 1: Contours of streamwise velocity and interface (blue line) for rectangular ducts of aspect ratio $L_x = 0.5$, $L_x = 2$ and $L_x = 5$, for the same mass flow rate over spanwise unit length, G_1/L_x and G_2/L_x.

This problem definition defines a nonlinear relation between four scalar quantities, h_{in},$S = \partial\bar{p}/\partial x$,G_1 and G_2. For given G_1 and G_2, h_{in} and S must be determined as part of the solution, together with the corresponding velocity field $u(x, y)$. A Newton method is used for the solution of the problem, that iterates on S and h_{in} until obtaining a velocity field that satisfies that the computed G_1 and G_2 are equal to the prescribed ones.

2.2 Linear Stability Analysis

A linear stability analysis based on the discretized version of the governing equations is considered here. The three-dimensional momentum equations, the continuity equation and the equation for the advection of the level function are simplified by introducing the flow decomposition (6) and the fully-developed flow hypothesis for the base flow. Linearized three-dimensional and time-dependent equations for the perturbations are obtained by subtracting the equations governing the base flow and neglecting quadratic terms on the disturbance. The latter is based on the infinitesimally small amplitude of the disturbances in the initial stages of growth, and is an usual assumption in stability analyses.

The linearized equations for a base flow dependent on two out of the three spatial directions are homogeneous in the third, streamwise direction and on time. Without loss of generality, the modal form

$$\mathbf{q}'(x, y, z, t) \sim \hat{\mathbf{q}}(y, z) \exp\left[\mathrm{i}(\alpha x - \omega t)\right] \tag{9}$$

is introduced for the disturbances. Substituting (9) on the governing equations and reordering terms, the generalized eigenvalue problem for the modal instability analysis is obtained in the form

$$\mathrm{i}\omega \mathbf{B}\hat{\mathbf{q}} = \mathbf{A}(\alpha, Re, We, Fr, \bar{\mathbf{q}})\hat{\mathbf{q}}. \tag{10}$$

For given parameters Re, We, Fr and base flow $\bar{\mathbf{q}}$, determined following the procedure in the previous section, the matrix eigenvalue problem (10) relates the values of the streamwise wavenumber α and the frequency ω for different families of possible linear waves.

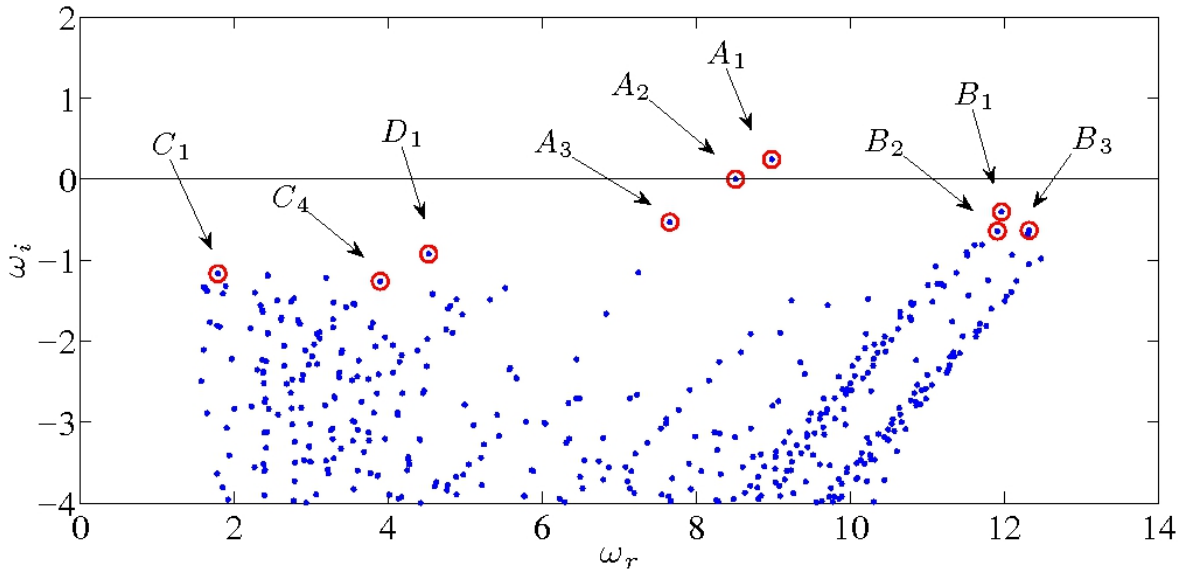

Figure 2: Eigenvalue spectrum corresponding to the linear stability problem, for a rectangular duct with aspect ratio $L_x/L_y = 1$, for $\alpha = 5$, which corresponds to a wavelength $\lambda \approx 1.25 L_y$.

In the temporal instability analysis, α is a real value corresponding to a streamwise periodicity length, and the eigenvalues are complex ω values, the real part ω_r of which corresponds to the circular frequency and the imaginary part ω_i to the temporal growth rate. If $\omega_i > 0$ for one eigenmode, then its amplitude will grow with time and the base flow is unstable. Stability of the base flow requires that $\omega_i < 0$ for all the eigenmodes.

3. NUMERICAL METHODS

The two-dimensional partial differential equations corresponding to both the computation of the base flow (7) and the linear stability eigenvalue problem (10) are discretized using sixth-order finite differences. For numerical reasons, the Heaviside and Dirac's functions are replaced in the computations by smoothed functions, following Sussman *et al.* (1994). The width of the resulting smoothed interface is chosen to be twice the grid spacing.

The eigenvalue problem (10) is solved using an in-house implementation of the shift-and-invert Arnoldi algorithm. This Krylov's subspace iteration allows the computation of an arbitrarily large window of the eigenspectrum at a small fraction of the cost of alternatives like the QZ algorithm.

Matrix operators are formed and operated on in sparse format. In-house routines are used for matrix-vector and matrix-matrix operations, while the ordering library METIS and the multifrontal solver library MUMPS (Amestoy *et al.* (2001)) are used for the computation of LU decompositions and back-substitutions. The use of sparse storage and operations reduces drastically the computational resources required for the solution as compared to an equivalent dense-algebra computation (Gennaro *et al.* (2013)). Required memory is reduced by an order of magnitude, while CPU is reduced further, thus allowing the computations to be done in a laptop computer and in times of minutes.

4. RESULTS

To illustrate the capabilities of the proposed methodology, parameters from the simulation of an oil-water channel flow are taken from Gada and Sharma (2012). The dimensional parameters employed by them are: $\rho_1^* = 819.25$ Kg m^{-3}, $\mu_1^* = 4.75 \cdot 10^{-3}$ Pa s, $\rho_2^* = 997.85$ Kg m^{-3}, $\mu_2^* = 0.89 \cdot 10^{-3}$ Pa s, $D^* = 2.8$ mm, resulting in $\chi = 1.218$ and $\eta = 0.1874$. The gravity constant is $g = 9.81$ m s^{-2}. They impose the mass flow rate in an indirect manner, in order to compute with numerical simulations: they assume an uniform velocity profile at entry, in which the two phases have velocity U_{in}^*, and the ratio is determined by the entry water level h_i. The case with $U_i^* = 0.5$ m s^{-1} is considered here. With the current dimensionless form $Re = 241.5$, $Fr = 3.017$, and $We = 9.22$.

4.1 Base flow computations

The approach is validated by recovering asymptotically the velocity profile corresponding to the two-dimensional channel when the aspect ratio is very large. In a first step, to eliminate numerical uncertainties, this algorithm is applied to the computation of the one-dimensional velocity profile and compared with the analytical solution. Then the solution is computed for rectangular ducts with increasing aspect ratio (L_x). In order to make the cases comparable, the mass flow rates corresponding to the channel are multiplied with L_x. Table 1 shows the streamwise pressure gradient, interface height and peak velocity as a function of L_x. Numerical computations are done using 201 equispaced points in the vertical direction, and 121 points in the horizontal direction with a mapping clustering points at the boundaries.

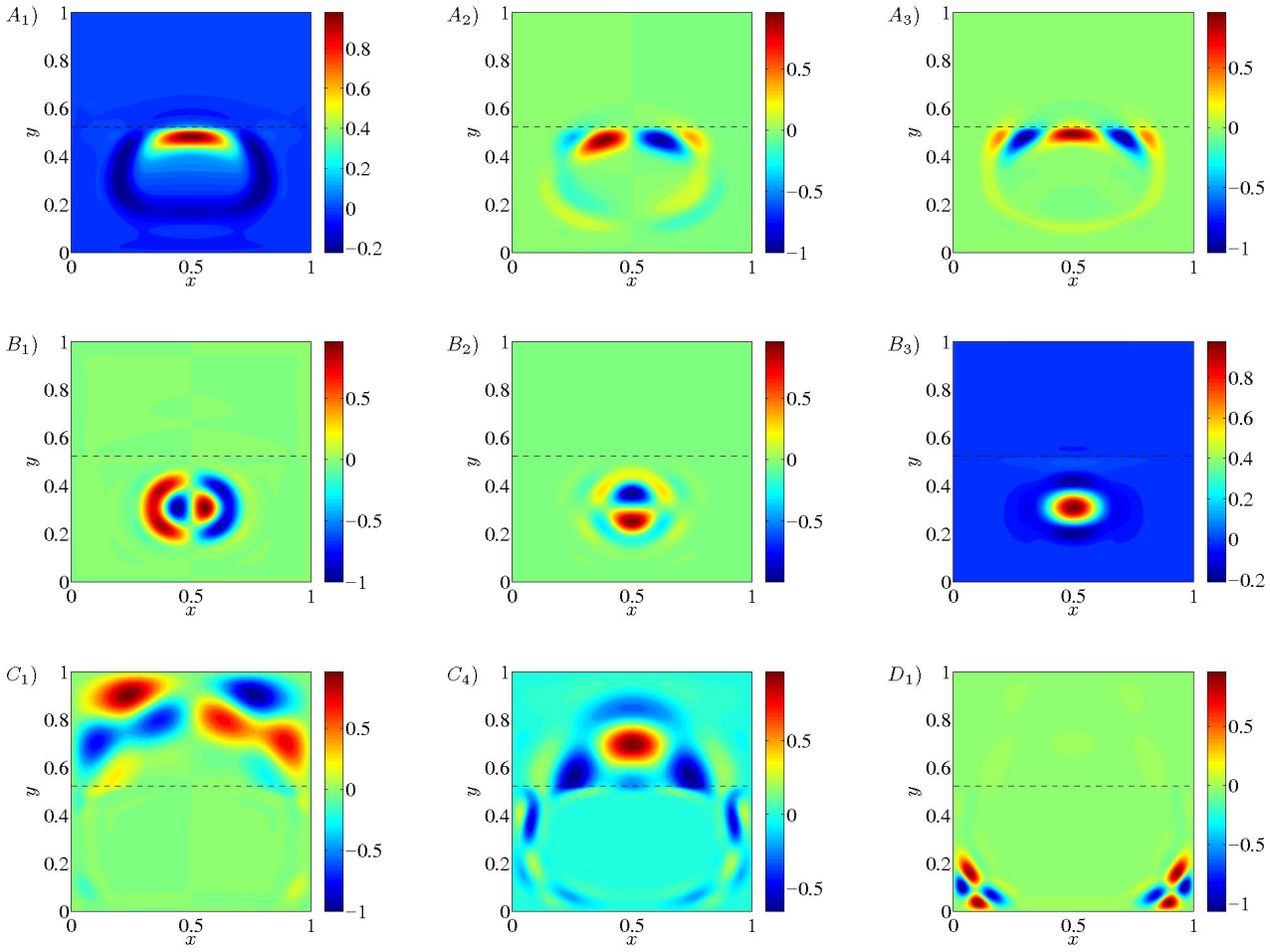

Figure 3: Streamwise velocity component $\hat{w}$ corresponding to representative eigenmodes for a rectangular duct with aspect ratio $L_x/L_y = 1$, for $\alpha = 5$, highlighted in figure 2.

4.2 Linear stability analysis

Figure 2 shows a representative eigenspectrum resulting from the solution of the generalized eigenvalue problem (10) for the base flow corresponding to $L_x = 1$ and streamwise wavenumber $\alpha = 5$. A resolution of $N_x \times N_y = 121 \times 201$ is used. Using the shift-and-invert Arnoldi's algorithm, the window of the 1500 eigenvalues closer to $\mu = 6 + \mathrm{i}0$ is computed. Unstable spurious eigenvalues within the window were identified by comparing with a higher resolution and by visual inspection of the eigenfunctions, and consequently were eliminated from the eigenspectrum.

Several branches of eigenmodes are identified, that can be related to the branches appearing in the eigenspectrum corresponding to the two-phase plane channel flow (cf. South and Hooper (1999)). As was shown in table 1, the rectangular-section base flow properties converge towards the infinite-span channel as aspect ratio is increased. Consequently, the instability eigenspectrum for three-dimensional perturbations should be expected to contain approximations to the plane eigenmodes of the one-dimensional flow, plus an infinite number of additional discrete modes accounting for the more stable oblique eigenmodes and the effect of the lateral walls.

Figure 3 shows the eigenfunctions recovered for the rectangular duct, for eigenmodes representative of the main branches. Eigenmodes A_1, A_2 and A_3 correspond to interfacial waves, in decreasing order of temporal growth rate. Each consecutive eigenmode introduces an additional pseudo-wavelength along the x-direction, thus corresponding to oblique waves of increasing angle with the streamwise direction. These eigenmodes being unstable, infinitesimal-amplitude disturbances that excite them will grow in amplitude according to their spatial structure and complex frequency and give rise to finite-amplitude interfacial waves, as shown, for example, in Garcia *et al.* (2016).

Eigenmodes B (B_1, B_2 and B_3) are the leading eigenmodes corresponding to internal waves within the denser water phase. Similarly, eigenmodes C corresponds to the leading internal waves in the lighter oil phase; the subsequent eigenmodes within their branches have a similar structure, introducing pseudo-wavelengths both in the x and y directions. Eigenmodes in these branches are always stable for newtonian flows, but can result in important transient energy growths if adequately perturbed, as shown for plane channels by $SouthandHooper$ (1999).

Additional eigenmodes can be identified in the eigenspectrum; though they are not relevant for the physics under the particular combination of parameters chosen, they might become important for other cases. One example is mode D_1 highlighted in the eigespectrum (fig. 2) and whose spatial structure is shown in figure 3. This is a corner eigenmode,

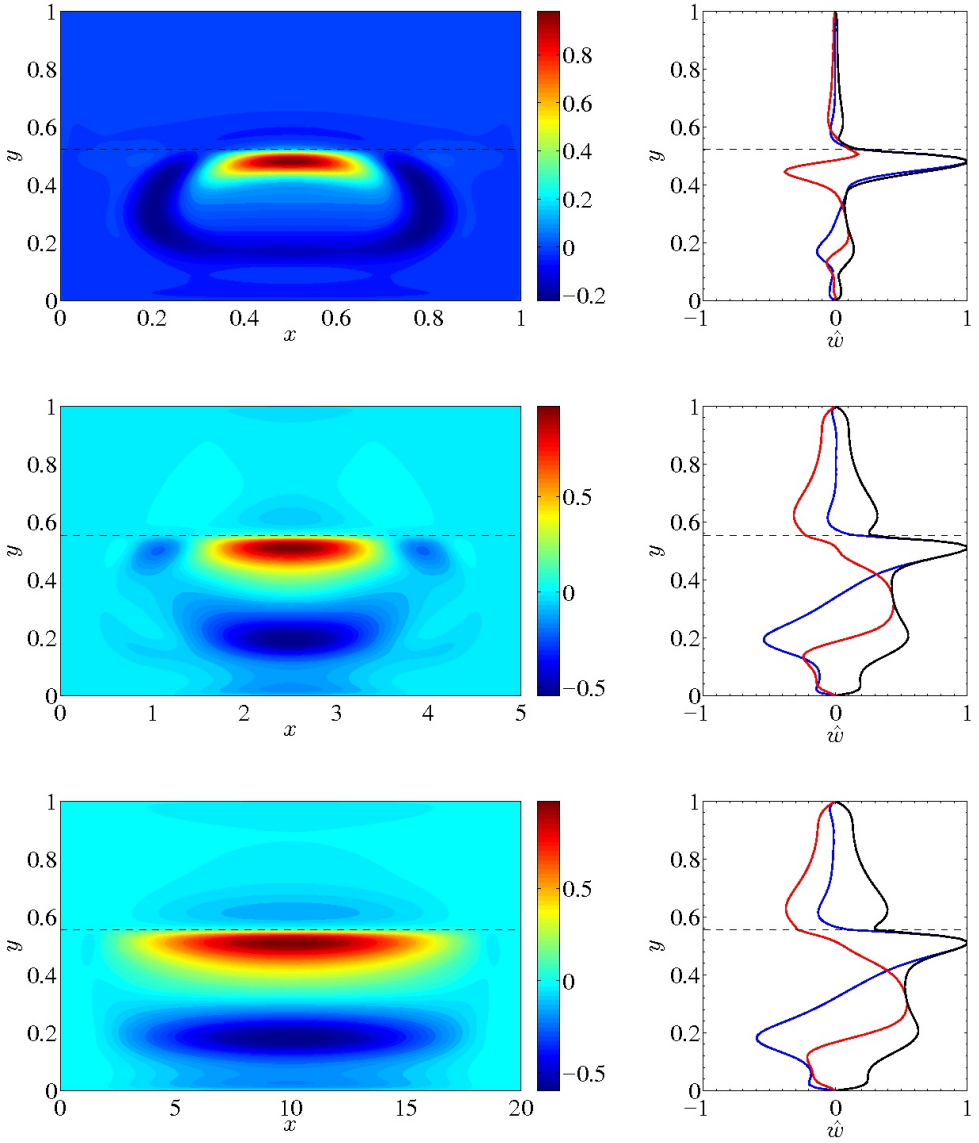

Figure 4: Streamwise velocity component $\hat{w}$ of the leading interfacial instability eigenmode, for three aspect ratios, $L_x/L_y = 1, 5$ and 20, and $\alpha = 5$. Left: isocontours of the cross-plane eigenfunction; Right: Real (blue), imaginary (red) and absolute (black) components of $\hat{w}$ at the channel cross-section.

internal to the heavier phase. The physical mechanism responsible to corner modes is analogous to the wall-modes in flat-plate boundary layers and is dominated by viscosity. Under certain conditions, defined by particular ranges of the parameters α, Re, r, m and $\bar{W}_{max}$, these corner eigenmodes can become temporally amplified, being one possible trigger for laminar-turbulent transition of its corresponding phase.

The effect of the aspect ratio on the interfacial instability eigenmodes is addressed now. Figure 4 shows the streamwise velocity fields corresponding to the leading interfacial instability eigenmodes, for ducts with aspect ratio $L_x/L_y = 1$, 5 and 20. The resolution in the x direction has been increased up to $N_x = 351$ to ensure convergence of results for the largest aspect ratio. Note that the x direction has been rescaled in the figures, to allow for comparison of the corner effects on the eigenmode. The importance of corner effects, associated with the effect of the lateral walls, decrease fast as the aspect ratio is increased. For L_x/L_y above 5, the dissipative influence of the lateral walls is very small, and the differences observed on the eigenvalues corresponding to the leading eigenmodes are primarily related to the difference in the base flow interface height. As $L_x/L_y \to \infty$, the instability velocity profile converges towards the one corresponding to the classic one-dimensional analysis for the plane-channel flow (Renardy, 1987; South and Hooper, 1999; Garcia *et al.*, 2016).

5. CONCLUSIONS AND FUTURE DIRECTIONS

This contribution presented the most recent steps towards the development of a new approach for the prediction of transition from a smooth-interface, gravity stratified two-phase flow to wavy interface and slug formation regimes in ducts and pipes of arbitrary cross-section. From a theoretical point of view, this new methodology requires of efficient

methods for the calculation of fully-developed flows along ducts and pipes, and of an approach that enables extending the classic methods for linear stability analysis, devised for one-dimensional base flows, to more complex flows depending on multiple spatial directions. These two tasks are accomplished here for flow along rectangular sections, and be extended in a straight-forward manner to arbitrary cross-sections.

The use of an optimized combination of variable-stencil high-order finite differences along with sparse algebra and storage and the Arnoldi's algorithm results into a computational cost reduction of some orders-of-magnitude with respect to the combination of a Chebyshev discretization, dense storage and QZ algorithm combination typically used in the literature for one-dimensional problems Renardy (1987); Boomkamp and Miesen (1997); South and Hooper (1999). The result is that one-dimensional problems with spatial resolution $N_y \sim 250$ can be solve in times of few seconds, and two-dimensional problems with resolutions $Nx \times N_y \sim 121 \times 201$ in times of minutes in a laptop computer.

Ongoing developments are focused on the implementation of a high-order immersed interface method in the spatial discetization, that enables the study of stratified flow in arbitrary-section pipes and ducts.

6. ACKNOWLEDGEMENTS

This work is funded by the Science without borders/CAPES- "Attraction of Young Talents" Fellowship and São Paulo Research Foundation (FAPESP) grant 2014/24782-0.

7. REFERENCES

Amestoy, P.R., Duff, I.S., L'Excellent, J.Y. and Koster, J., 2001. "A fully asynchronous multifrontal solver using distributed dynamic scheduling". *SIAM J. Matrix Anal. Appl.*, Vol. 23, No. 1, pp. 15–41. ISSN 0895-4798.

Barnea, D. and Taitel, Y., 1993. "Kelvin-Helmholtz instability criteria for stratified flow: viscous versus non-viscous (inviscid) approaches". *Int. J. Multiphase Flow*, Vol. 19, No. 4, pp. 639–649.

Boomkamp, P.A.M. and Miesen, R.H., 1997. "Classification of instabilities in parallel two-phase flow". *Int. J. Multiphase Flow*, Vol. 22, No. Suppl, pp. 67–88.

Gada, V.H. and Sharma, A., 2012. "Analytical and level-set method based numerically on oil-water smooth/wavy stratified-flow in an inclined plane-channel". *Numer. Heat Transfer B*, Vol. 56, pp. 307–322.

Garcia, D.E., Rodríguez, D., de Paula, I.B. and Nieckele, A.O., 2016. "Linear stability analysis of stratified two-phase flow in a plane channel using numerical simulation". 16th Brazilian Congress of Thermal Sciences and Engineering - ENCIT, November 7-10th, Vitória ES, Brazil.

Gaster, M., 1962. "A note on the relation between temporally-increasing and spatially-increasing disturbances in hydrodynamic stability". *J. Fluid Mech.*, Vol. 14, pp. 222–224.

Gennaro, E.M., Rodríguez, D., Medeiros, M.A.F. and Theofilis, V., 2013. "Sparse techniques in global flow instability with application to compressible leading-edge flow". *AIAA J.*, Vol. 51, No. 9, pp. 2295–2303.

Lin, P. and Hanratty, T., 1986. "Prediction of the Initiation of Slugs with Linear Stability Theory". *Int. J. Multiphase Flow*, Vol. 12, No. 1, pp. 79–98.

Renardy, Y., 1987. "Then thin-layer effect and interfacial stability in a two-layer Couette flow with similar liquids". *Physics of Fluids*, Vol. 30, No. 6, pp. 1627–1637.

South, M.J. and Hooper, A.P., 1999. "Linear growth in two-fluid plane poiseuille flow". *J. Fluid Mech.*, Vol. 381, pp. 121–139.

Sussman, M., Smereka, P. and Osher, S., 1994. "A level set approach for computing solutions to incompressible two-phase flow". *J. Comp. Phys.*, Vol. 114, pp. 146–159.

Taitel, Y. and Dukler, A., 1976. "A Model for predicting flow Regime transitions in horizontal and near horizontal gas-liquid flow". *A. I. Ch. E.*, Vol. 22, pp. 47–55.

8. RESPONSIBILITY NOTICE

The author(s) is (are) the only responsible for the printed material included in this paper.